

AD-A048 687

BROWN UNIV PROVIDENCE R I DIV OF ENGINEERING
EXPERIMENTS ON DYNAMIC PLASTIC LOADING OF FRAMES.(U)
JUL 77 S R BODNER , P S SYMONDS

F/G 13/13

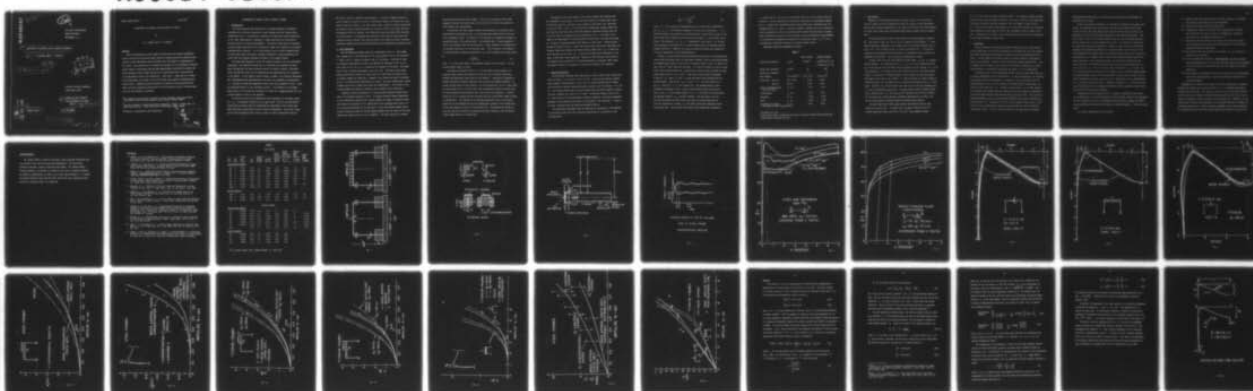
N00014-75-C-0860

UNCLASSIFIED

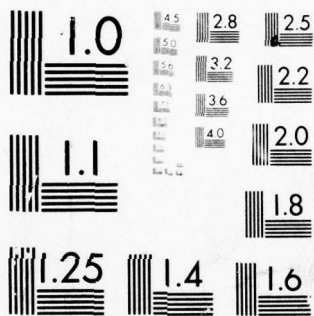
N00014-0860/4

NL

| OF |
AD
A048687



END
DATE
FILMED
2-78
DDC



MICROCOPY RESOLUTION TEST CHART
NATIONAL BUREAU OF STANDARDS-1963-A

AD A 048687

NR 064-1124
note - 474

12

Division of Engineering

BROWN UNIVERSITY

PROVIDENCE, R. I.

6

EXPERIMENTS ON DYNAMIC PLASTIC LOADING OF FRAMES.

10

S. R. Bodner and P. S. Symonds

12 41 p.

9

Technical rept.,

DDC
JAN 16 1978
RECEIVED
F

National Science Foundation

Grant ENG74-21258

15

Office of Naval Research

Contract N00014-75-C-0860,

VNSF-Eng-74-21258

11

July 1977

14

N00014-0860/4

AD NO. FILE COPY
DDC

DISTRIBUTION STATEMENT A
Approved for public release
Distribution Unlimited

065 310 mt

EXPERIMENTS ON DYNAMIC PLASTIC LOADING OF FRAMES

I. Introduction

The tests described here were part of a research program on estimation techniques for structures subjected to pulse loading such that large plastic deformations occur. In particular, extensions of deflection bound theorems and of the "mode approximation" technique to large deflections and viscoplastic material behavior are being investigated. The present tests were on structures in which large deflections do not drastically change the stiffness, the response remaining mainly flexural. In the same program, tests on fully clamped plates [1] were made, where the greatly increased stiffness at large deflections contrasts with the slightly decreased stiffness in the present frames.

The tests were designed to study the overall accuracy of the two estimation techniques. The deflection bounds and the deflection and response time estimates furnished by the mode technique involve two kinds of errors, "intrinsic" errors and further errors due to idealizations and approximations not essential to the method. In the present tests we hoped to assess their relative importance. The "idealizations and approximations" are almost all regarded as conservative, i.e., leading to deflection magnitudes larger than those expected in tests. These are discussed further in the concluding section. Full details of the present applications of the estimation techniques are given in a companion paper [2], but a brief summary is given in the Appendix.

The intrinsic error in the deflection bound technique is, of course, positive, i.e., the computed deflection is an upper bound. That in the mode method arises from the device used for determining the amplitude of the initial mode form field from the specified initial velocity distribution. This error is negative if the specified initial velocity field is "more concentrated" than the

mode shape, positive otherwise (see Appendix). In order to compare these, we used two types of loading, one with a concentrated impulse, the other with a uniformly distributed impulse. For each loading type, a range of impulse intensities was applied, giving final deflections up to about a third of the span, the basic measurements being the impulse, final deflected shape, and strain-time histories at several points. This program was carried out for frames for mild steel and commercial purity titanium, both having strongly rate sensitive plastic behavior. Parameters characterizing the material behavior were established by separate tests.

2. Test Techniques

The two frames and loading types are illustrated in Fig. 1. Both frames have columns 8.0 in. long and span 12.0 in. long, width 0.750 in. and thickness H about 0.123 in. (steel) and about 0.092 in. (titanium). The frame of type (a) enabled a concentrated impulse to be applied as indicated in Fig. 1a to a steel block $3/4$ in. by 1.5 in. attached at the midpoint of the span. The frame type (b) had a uniform beam member, as in Fig. 1(b). The feet of the column members were fixed in slots in a steel block of 3 inch depth, as shown, so as to provide clamped end conditions. Corners of the frames are shown in sketches of Fig. 2 to indicate the fabrication techniques. The steel frames used a silver soldered joint with a square brass piece for reinforcement. The corners of the titanium frames were joined by welding, using titanium as the weld metal.

Explosive loading was applied by detonating sheet explosive (Dupont Deta-sheet C) of nominal thickness 0.08 in. To obtain different impulse magnitudes in the concentrated impulse tests, varying numbers of layers of explosive sheet were fixed to the central $3/4$ in. square area of the attached block over a $1/4$ in. thick pad of Neoprene of the same area. In the distributed impulse tests, strips of explosive sheet of various widths extended over the length of the beam member over buffer strips of $1/8$ in. Neoprene. The buffer pads act to reduce

peak pressures and reduce local damage. The mass of the pads was very small compared to either the central mass or the mass of the beam so the effect of their inertia was insignificant.

In each test the total impulse applied was measured by the ballistic pendulum device [3] sketched in Fig. 3, the specimen base being bolted on one end of the suspended I-beam. The impulse on the specimen is transmitted through its supporting frame to the pendulum mass. The pendulum mass is large compared to that of the specimen, and its natural period is long compared to the duration of the specimen response or of the pressure pulse. Very accurately, the impulse I is obtained from the maximum displacement X_m of the pendulum at its mass center by

$$I = \frac{W}{g} \frac{2\pi}{T} X_m \quad (1)$$

where W is the total weight of the pendulum (about 75 3/4 lb) and T is its natural period (about 3.3 sec).

The impulse calculated from Eq. (1) is the correct total impulse on the specimen frame provided the pendulum is acted on only by forces transmitted through the designated loading area of the specimen. Shielding is necessary to prevent extraneous impulsive pressures from reaching the pendulum directly or acting on other areas of the specimen. The main shield was a 1/4 in. steel plate as illustrated in Fig. 2 for the tests with concentrated impulse; for each type of test an aperture fitted closely the loaded area of the specimen. A second shield of 3/4 in. plywood also was inserted since the first shield cannot provide a complete seal. The impulse on the specimen depends not only on the charge weight but on its geometry and on the configuration adjacent to the loaded area; it may also depend on details of the specimen [4]. We measured the impulse in each test instead of relying on calibration factors, keeping a plot of impulse versus charge weight as a rough check.

Information on the time history of the frame response was obtained from wire resistance strain gages. These were SR-4 gages of 1/4 gage length (type FAE-25-12S6) placed at the tops of the columns on both sides, with locations as shown in Figs. 1 and 2. In the tests with concentrated impulse, gages were also placed on the back side of the beam member at distances ranging from 1/8 to 3/8 in. from the attached block as indicated in Fig. 2. We tried to put gages on the beam member in the distributed impulse tests, but these all failed as a result of strong thickness wave effects in these tests. Typical strain records are shown in Fig. 3. Apart from giving strain and strain rate data, two response times were obtained from these records, namely time t'_f to reach the first maximum, and the time t''_f at which the rising signal intersects a line drawn at the final strain magnitude. Neither of these directly corresponds to the response time calculated in the mode approximation technique, where rigid-viscoplastic behavior is assumed, but they are of interest for comparison.

3. Material Properties

The mild steel specimens were made from hot rolled carbon steel (C1008) supplied as strips 1 in. by 1/8 in. by 10 ft long. They were used without further heat treatment, being milled to width 0.750 in. before fabricating the frames. The thickness as supplied showed negligible variation from the average $H = 0.123$ in. The titanium frames were made from commercially pure (99.2 percent) titanium (Ti-50A), supplied as a sheet of 4 ft width. To make the frames, strips 0.750 in. wide were cut in the longitudinal (rolling) direction, and tensile properties measured in this direction were used in the analyses. The thickness H varied by about 1 percent above and below the average 0.0918 in.

The estimation techniques treat the material as viscoplastic, with behavior in the plastic range that can be described adequately by an equation of the following form:

$$\frac{\sigma}{\sigma_0} = 1 + \left(\frac{\dot{\epsilon}}{\dot{\epsilon}_0} \right)^{1/n} \quad (2)$$

where σ , $\dot{\epsilon}$ are stress and corresponding plastic strain rate, respectively, and σ_0 , $\dot{\epsilon}_0$, n are material parameters of strain rate sensitivity. σ is generally taken as the stress at a specified plastic strain level in test at constant strain rate; however for mild steel we have taken σ as the lower yield stress. The constants σ_0 , $\dot{\epsilon}_0$, n correspond to this choice. Eq. (2) generally provides an excellent fit in a least squares sense for strongly rate dependent metals [8]. (However, it should be noted that strain rate history effects are disregarded in this representation.)

Ideally, we should have made tensile stress-strain tests on our materials at strain rates from quasi-static to magnitudes exceeding those in the tested frames; the maximum strain rates in the tests were probably about 50 sec^{-1} so tests to at least 100 sec^{-1} would have been desirable. To avoid the expense of tests at high strain rates we made tests with a conventional testing machine (Instron) at four strain rates from 10^{-4} to 0.1 sec^{-1} . From each of these tests we computed a value of σ_0 , using $\dot{\epsilon}_0$ and n values determined from published data on similar metals. Thus we took $\dot{\epsilon}_0 = 40 \text{ sec}^{-1}$, $n = 5$ for mild steel [5, 6] and $\dot{\epsilon}_0 = 120 \text{ sec}^{-1}$, $n = 9$ for titanium [7]. The determination of these constants is discussed in [8]. Typical stress-strain curves are shown in Figs. 5 and 6. If the assumed values of $\dot{\epsilon}_0$, n are valid for our materials, the measured values of σ_0 would be constant. This was found to be the case for mild steel; the four strain rate tests on coupons from any one 10-ft bar furnished an average σ_0 with small scatter and negligible trend with strain rate. For nine bars from which tested frames were fabricated,

σ_0 varied from 32.0 to 33.8 ksi; the average value 33.1 ksi was used in the calculations. For our titanium, the four strain rate tests on longitudinal coupons gave σ_0 values which increased slightly with strain rate, indicating that the assumed values of $\dot{\epsilon}_0$ and n were less suitable. However, the r.m.s. deviation from the average 35.2 ksi (at 1 percent plastic strain) was only about 3 percent. Strain hardening was larger for this material, and was accounted for approximately in the estimation techniques by repeating the calculation using $\sigma_0 = 37.7$ ksi, corresponding to measured stresses at 2 percent plastic strain.

Numerical values are summarized in Table 1.

Table 1

		Steel Frames	Titanium Frames
Strain rate constant ¹	σ_0 psi	33,100 ²	35,200 ³ at $\epsilon^p = 1\%$ 37,700 ³ at $\epsilon^p = 2\%$
Strain rate constant ¹	$\dot{\epsilon}_0$ sec ⁻¹	40	120
Strain rate constant ¹	n	5	9
Mass density	ρ lb sec ² in. ⁻⁴	0.73×10^{-3}	0.42×10^{-3}
Total span type (a)	$2L_1 + 2a$ in.	12.00	12.00
type (b)	$2L_1$ in.	12.00	12.00
Width of attached block (type (a) frame)	$2a$ in.	0.75	0.75
Column height	L_2 in.	8.00	8.00
Thickness	H in.	0.123	0.092
Width	b in.	0.750	0.750
Attached block weight (including enclosed beam section)	G lb	0.21	0.21

¹As used in Eq. (2).

²Lower yield stress; average for nine bars, from four strain rates for each bar.

³Longitudinal (rolling) direction.

4. Test Results

Examples of final deflected shapes are shown in Figs. 7-10 for the two types of loading and the two materials; these are typical of large deflection results, with maximum displacement on the order of a third of the span dimension. The curves were traced from the deformed frame before removal from the support base.

The main deflection is that of the midpoint of the beam member, labelled w_c^f , and shown in Figs. 11, 12, 14, 15 as a function of the impulse I . A secondary deflection magnitude is the inward motion of the corner, marked u_B^f in Figs. 7-10. This is shown in Figs. 13 and 16 as function of I . The quantity plotted is the average for the two corners, the deformation being slightly unsymmetric in some cases. The test data are summarized in Table 2.

In Figs. 17-20 are shown the measured response times t_f' and t_f'' plotted against impulse. As illustrated in Fig. 4, t_f' is the peak response time and t_f'' is the time at which the final strain magnitude is first reached; i.e., it is the intercept of a line drawn at the final strain level with the rising strain signal. In the tests on titanium frames, strain records were obtained mainly from gages at the tops of the columns. At these locations the plastic strain is relatively small, and the record does not furnish the intercept time t_f'' accurately. Hence in Fig. 18 test results are shown only for the peak response time t_f' for the concentrated mass tests. The gage records showed a plateau rather than a distinct peak; t_f' was taken as the time when this was first reached. For the tests with uniform impulse, meaningful determination of either time did not seem possible, probably because of strong elastic effects.

The most informative strain gage records were obtained for the steel frames with central mass. In these tests, the gages near the top of the columns registered strain rates of 5 to 10 sec^{-1} and permanent strains

of 0.5 to 1.2% over the range of impulse values. The response of gages attached near the central mass depended critically on the exact location of the gage since the plastic straining was very localized. For test number 12 shown in Fig. 7 ($I = 0.715 \text{ lb sec}$) a strain gage placed $1/8 \text{ in.}$ away from the edge of the central mass indicated a strain rate of 30 sec^{-1} and a permanent strain of about 3 percent. These seem to be close to the maximum strain rates and strains experienced by the frame specimens in these tests.

5. Discussion

We are interested in comparing the measured deflections with upper bounds on the deflections, and the test deflections and response times with the approximate final deflections and durations obtained from the mode approximation technique. A brief summary of the main concepts of these estimation techniques is given in the Appendix. Details on their application appear elsewhere [2]. Here we compare the test results with those of the estimation techniques with particular attention to indications concerning the errors in the two approaches.

As already noted, we can distinguish between intrinsic errors and those due to further approximations and idealizations. In the bound approach, the intrinsic error arises from the substitution of a problem of static equilibrium for the original dynamic one; use of the theorem of minimum potential energy makes the intrinsic error positive, i.e., furnishes an upper bound. In the mode approach, the intrinsic error arises from the technique used to determine the magnitude of the initial mode velocity field from the initial velocity field. This gives the relation between the initial mode velocity amplitude \dot{w}_n^0 and the prescribed initial velocity \dot{w}_c^0 according to Eq. (A7) in the Appendix; their ratio is less than one for the concentrated impulse and greater than one for the uniformly distributed impulse. Thus the intrinsic error of the mode method is negative

(underestimates deflections) in the first case and positive (overestimates deflections) in the second.

If all the conditions underlying the estimation techniques were exactly satisfied, the comparison with test results would show the intrinsic error only. Figures 11 and 12 for steel frames would show test points above and below, respectively, the curve for the mode approximation (for finite deflections). Similarly Figs. 14 and 15 for titanium frames would show the test points above and below, respectively, the mode approximation curve. The actual test results do not show these relations consistently. Figures 11 and 12 do seem to be in fair agreement with expectations based on the intrinsic error, since in Fig. 11 the test deflections lie slightly above the estimated curve, and in Fig. 12 they are essentially on it. However, Figs. 14 and 15 (for titanium frames) show the opposite relations. For concentrated loading the observed deflections are too small, while for the distributed impulse tests they are only slightly below or on the curve for $\sigma_0 = 35$ ksi, and on or above the curve for $\sigma_0 = 38$ ksi. The two estimation curves are drawn in these figures as a way of taking rough account of strain hardening, which is more pronounced in titanium than in steel; the two values correspond to plastic strain 1% and 2%, respectively, in the determination of σ_0 from the strain rate tests. Agreement is better if $\sigma_0 = 38$ ksi is used, but the relation of test to estimated deflections remains opposite to what would occur if the intrinsic error dominated.

Explanations for this behavior must be sought by considering other errors in the application of the mode technique than the intrinsic error so far considered. For this calculation (and for the deflection bound as well) a number of idealizations were made, particularly with respect to material behavior. These are listed below:

- (1) Elastic deformations were neglected.

- (2) Plastic strain rates were written as explicit functions of stresses, with implicit consideration of strain hardening.
- (3) Strain rate history effects were neglected.
- (4) A homogeneous viscous stress-strain rate representation (without yield condition) was used in place of a homogeneous viscoplastic law, making use of matching technique [8, 9].
- (5) Essentially flexural behavior was assumed, the center-line strain being assumed zero, and axial forces disregarded in the constitutive equations (treated as reactions).
- (6) The pressure pulse was idealized as impulsive, i.e. as a finite impulse with zero duration.
- (7) In the extended mode technique, "instantaneous" mode form solutions were found appropriate to the current deflection field, and a succession of such solutions was made continuous only with respect to the major deflection.
- (8) The numerical determination of the static solution in the bound method and of mode form solutions in the mode technique was carried out by iterative schemes.

Arguments can be made [2] that almost all of the idealizations or approximations listed above lead to positive errors, i.e., to estimated deflections exceeding the actual ones. The neglect of axial forces in the yield condition, item (5), may be an exception; assuming center-line axial strain zero is equivalent to assuming a stronger structure than the actual one. However it is not clear whether requiring the deformation to be absorbed entirely by flexural deformations should lead to larger or smaller magnitudes of the major deflection. The constraints are not ones that require center-line strains to occur even at

very large deflections. This idealization was believed to cause negligible error, but no direct check of this is available. Similarly, the numerical determination of instantaneous mode form solutions by iterative schemes is believed very accurate in the present cases, since convergence was rapid throughout. The neglect of plastic strain rate history is believed to cause a positive error, but the experimental evidence (mainly from tests in which the strain rate is rapidly changed) is very slight.

The influence of elastic deformations, neglected in the constitutive equations used, is difficult to assess. A rule-of-thumb energy criterion for validity of this neglect is a large value of the ratio of input energy to a measure of the elastic strain energy capacity of the structure. If this ratio R is greater than about 6 in a simple one degree of freedom model, the neglect of elastic effects causes a positive error of about 15 percent. If this holds in the present frame structures, the impulse should exceed about 0.45 lb-sec in the tests with concentrated impulse and about 0.25 lb-sec in those with distributed impulse; the required impulse is marked on Figs. 11, 12, 14, 15. The importance of elastic effects as indicated by this energy criterion appears essentially the same for both the steel and the titanium frames. The tests on titanium frames with concentrated impulse in Fig. 14 do show exactly the relation to the estimated deflection curves (for large displacements) that one would expect if the main discrepancies are due to the neglect of elastic deformations. The steel frames under concentrated impulse (Figs. 11) show similar trends, but the test points fall on the estimated deflection curve at small impulse magnitudes, and lie above it at higher impulses (rather than approaching the calculated curve from below).

The measurements of final inward displacement at the two corners (averaged for each frame) are shown in Fig. 13 (steel) and Fig. 16 (titanium). Comparison

of these secondary deflection magnitudes with those predicted by the extended mode technique is of interest because this deflection is zero according to the mode technique for small deflections. The mode technique predicts these deflections reasonably well at the larger impulse values.

A possible "experimental" error, which could cause the steel test frames to deflect more than expected, is a weakening at the corners where the beam member is silver-soldered to the two columns. This seems unlikely, however, since silver soldering requires fairly low temperatures, and the joints are strengthened by brass blocks as shown in Fig. 2. Moreover, static tests [10] on steel frames fabricated in the same way failed to show weaker behavior, when loads at first yield, first hinge development, and plastic collapse were compared with the calculated loads using yield stress measured at strain rates approximating those of the frame tests (about 10^{-3} sec^{-1}). This explanation also must be rejected.

In conclusion, it can be said that the deflection upper bounds are verified by the tests, and that the extended mode approximation method leads to deflection estimates close to those observed in the tests on steel frames, and below or close to those measured in the tests on titanium frames. Corroboration was not obtained of the intrinsic error of the mode technique, and further investigation of the various additional sources of error is required. However, the closeness of predicted to test results suggests that practical use of the approximation techniques can be made before such investigations are completed.

Acknowledgements

Mr. George LaBonte, Technical Assistant, gave invaluable assistance with the explosive tests and the strain gage measurements. Mr. Duty Mowry, Technical Assistant, expertly fabricated the frames. Mr. Michael Chosak, Research Engineer, was helpful in connection with tests on material behavior. We express our appreciation to them, and we also thank Professor R. J. Clifton for making available funds from NSF Grant ENG75-01426 which enabled the test program on titanium frames to be completed.

References

1. Bodner, S. R. and Symonds, P. S., "Experiments on Viscoplastic Response of Circular Plates to Impulsive Loading," Technical Report of Brown University under Grant NSF 74-21258 and Contract N00014-75-C-0860.
2. Symonds, P. S. and Chon, C. T., "Large Viscoplastic Deflections of Impulsively Loaded Plane Frames," Technical Report of Brown University under Grant NSF 74-21258 and Contract N00014-75-C-0860.
3. Bodner, S. R., "Deformation of Rate Sensitive Structures Under Impulsive Loading," Engineering Plasticity (J. Heyman and F. A. Leckie, Editors), Cambridge University Press, pp. 77-91, 1968.
4. Duffey, Thomas A. and Key, Samuel W., "Experimental-Theoretical Correlations of Impulsively Loaded Clamped Circular Plates," Research Report SC-RR-68-210, April 1968, Sandia Laboratories.
5. Manjoine, M. J., "Influence of Rate of Strain and Temperature on Yield Stresses of Mild Steel," J. Appl. Mech., Vol. 11, pp. A211-A - 218, 1944.
6. Aspden, R. J. and Campbell, J. D., "The Effect of Loading Rate on the Elasto-Plastic Flexure of Steel Beams," Proc. of the Royal Society, A, Vol. 290, 266-285, 1966.
7. Hsu, J.C.C. and Clifton, R. J., "Plastic Waves in a Rate Sensitive Material-- Part I. Waves of Uniaxial Stress," J. Mech. Phys. Solids, Vol. 22, pp. 233 to 253, 1974.
8. Symonds, P. S. and Chon, C. T., "Approximation Techniques for Impulsive Loading of Structures of Time-Dependent Plastic Behavior With Finite Deflections," Proc. Oxford Conf., Mechanical Properties of Materials at High Strain Rates, Inst. of Physics Conf. Ser. No. 21, Dec. 21, 1974, pp. 299-315, Edited by J. Harding.
9. Symonds, P. S., "Approximation Techniques for Impulsively Loaded Structures of Rate Sensitive Plastic Behavior," SIAM J. Appl. Math., Vol. 25, No. 3, Nov. 1973, pp. 462-273.
10. Chon, C. T. and Symonds, P. S., "Large Dynamic Deflection of Plates by Mode Method," J. of the Eng. Mech. Div., Proc. ASCE, Vol. 103, No. EM1, pp. 3-14, Feb. 1977.
11. Exner, E., Mak, M., Moynihan, P., Pappas, J., and Wojcieszak, D., "Structural Analysis of a Clamped Portal Frame Under Static Point Loading," Project Report in Course EN 12, Spring 1976, Division of Engineering, Brown University.

TABLE 2

STEEL FRAMES

Test No.	Bar No.	Thick-ness H in.	σ_0 ksi	Charge Weight Grams	Impulse lb-sec	Final Deflec- tion at Center w_f in.	Final Deflec- tion Top of Column u_B^f in.	Time to Reach Max. Strain t_f' msec.	Inter- cept Time t'' msec
<u>Concentrated Impulse</u>									
S2	5	0.123	33.3	2.1	0.542	1.70	0.31	7.0	4.5
S3	5	0.123	33.3	2.6	0.61	2.03	0.430	7.8	5.4
S5	4	0.123	32.0	1.3	0.303	0.52	0.047	4.0	2.0
S6	8	0.123	33.8	1.6	0.40	0.83	0.094	5.0	3.0
S8	6	0.123	33.5	4.2	0.75	3.52	1.18	10.0	6.4
S9	6	0.123	33.5	3.7	0.71	3.06	0.89	9.0	-
S12	9	0.123	33.4	3.4	0.715	2.90	0.84	9.0	6.0
S13	3	0.123	33.15	2.8	0.66	2.59	0.68	-	-
<u>Uniform Impulse</u>									
S10	7	0.123	33.1	2.4	0.505	1.125	0.15	4.0	2.0
S11	7	0.123	33.1	3.65	0.79	2.83	0.78	6.5	4.2
S14	9	0.123	33.4	3.1	0.70	2.23	0.49	-	-

TITANIUM FRAMES

<u>Concentrated Impulse</u>									
T1		0.0911	35.0*	1.16	0.34	0.6	0.03	6	
T2		0.0913	35.0	2.1	0.56	3.09	0.92	8	2 (?)
T3		0.0928	35.0	2.2	0.575	3.25	0.94	8	2 (?)
T4		0.0927	35.0	1.65	0.492	2.03	0.41	7	2 (?)
T5		0.0902	35.0	2.6	0.66	5.12	2.34	8.5	3 (?)
T9		0.0925	35.0	1.4	0.47	1.83	0.33	7	2 (?)
T12			35.0	1.2	0.355	0.68	0.03	6.5	2 (?)
<u>Uniform Impulse</u>									
T6		0.0905	35.0	2.6	0.623	7.56	4.42		
T7		0.0914	35.0	1.4	0.323	1.34	0.20		
T8		0.0920	35.0	2.0	0.466	3.34	0.95		
T11		0.0894	35.0	1.7	0.336	1.80	0.34		

* At 1 percent strain; for 2 percent strain $\sigma_0 = 38.0$ ksi.

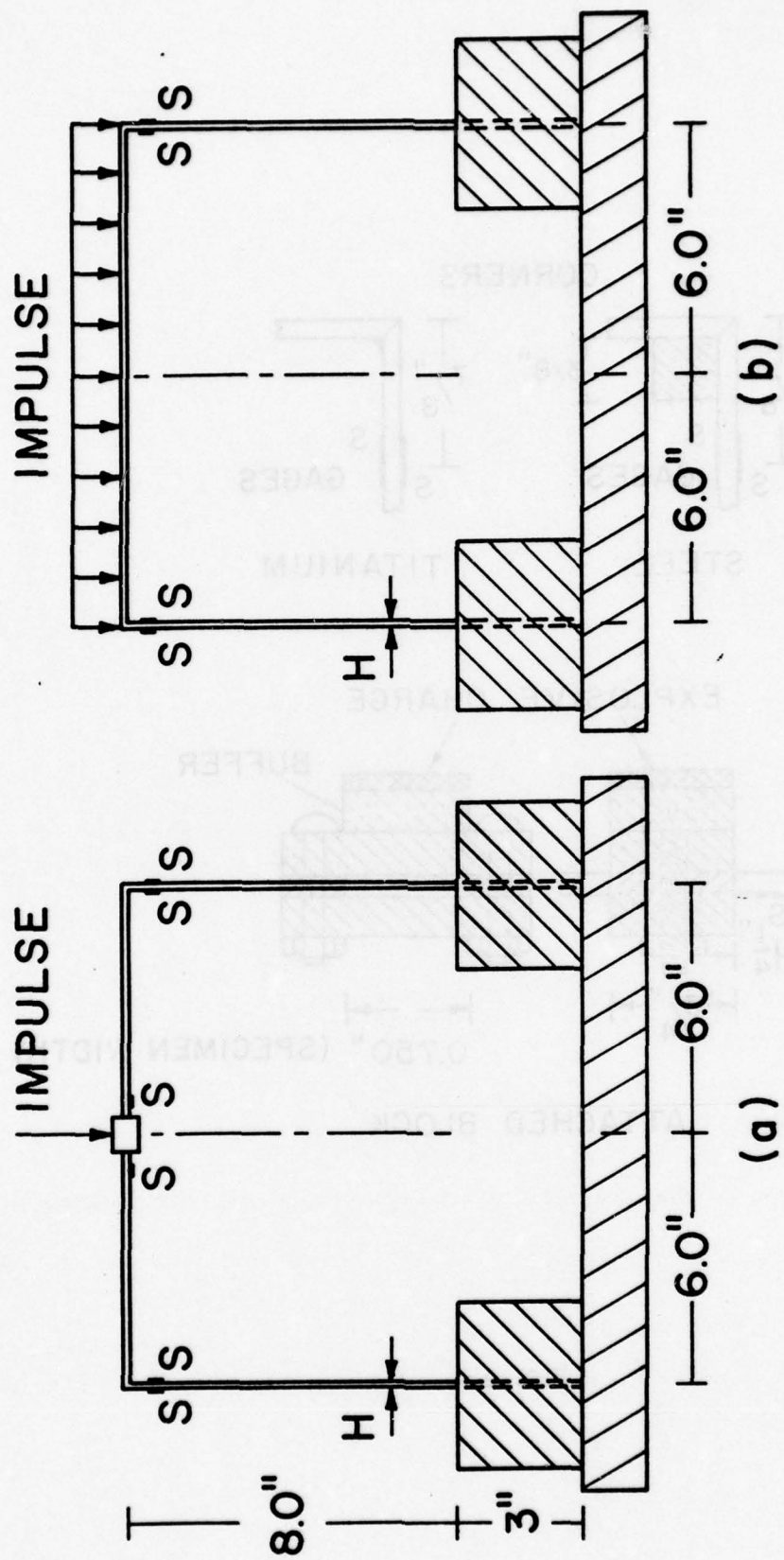


FIG. 1

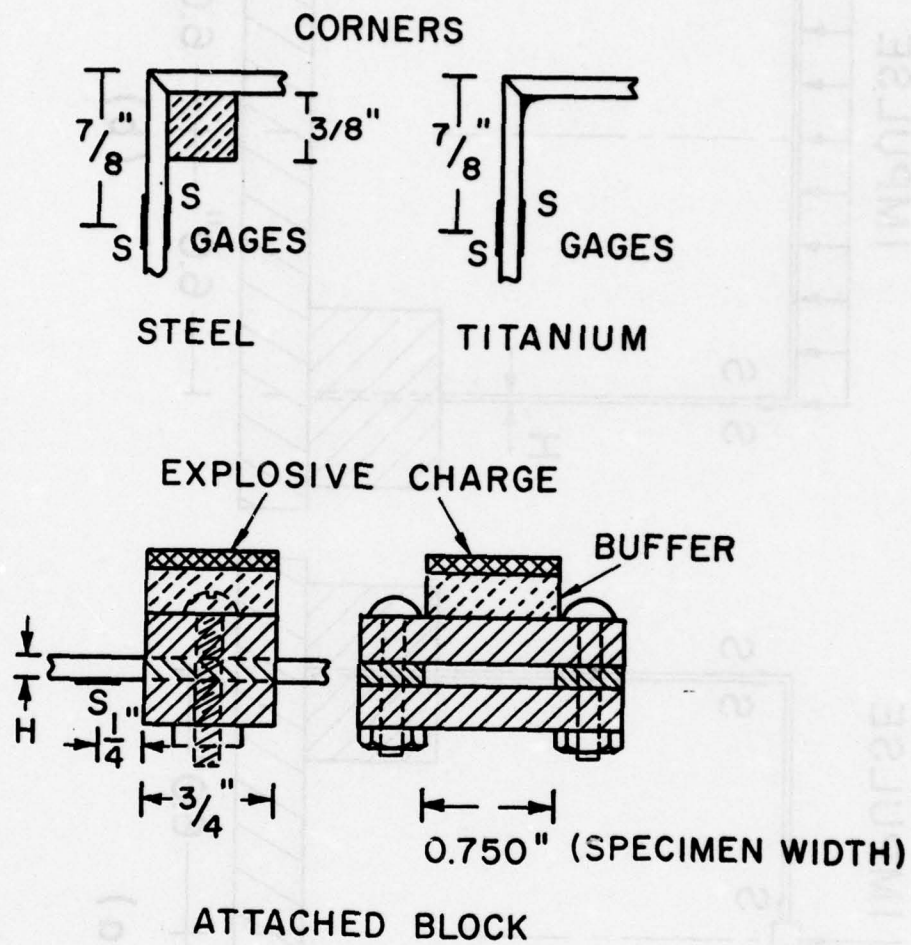


FIG. 2

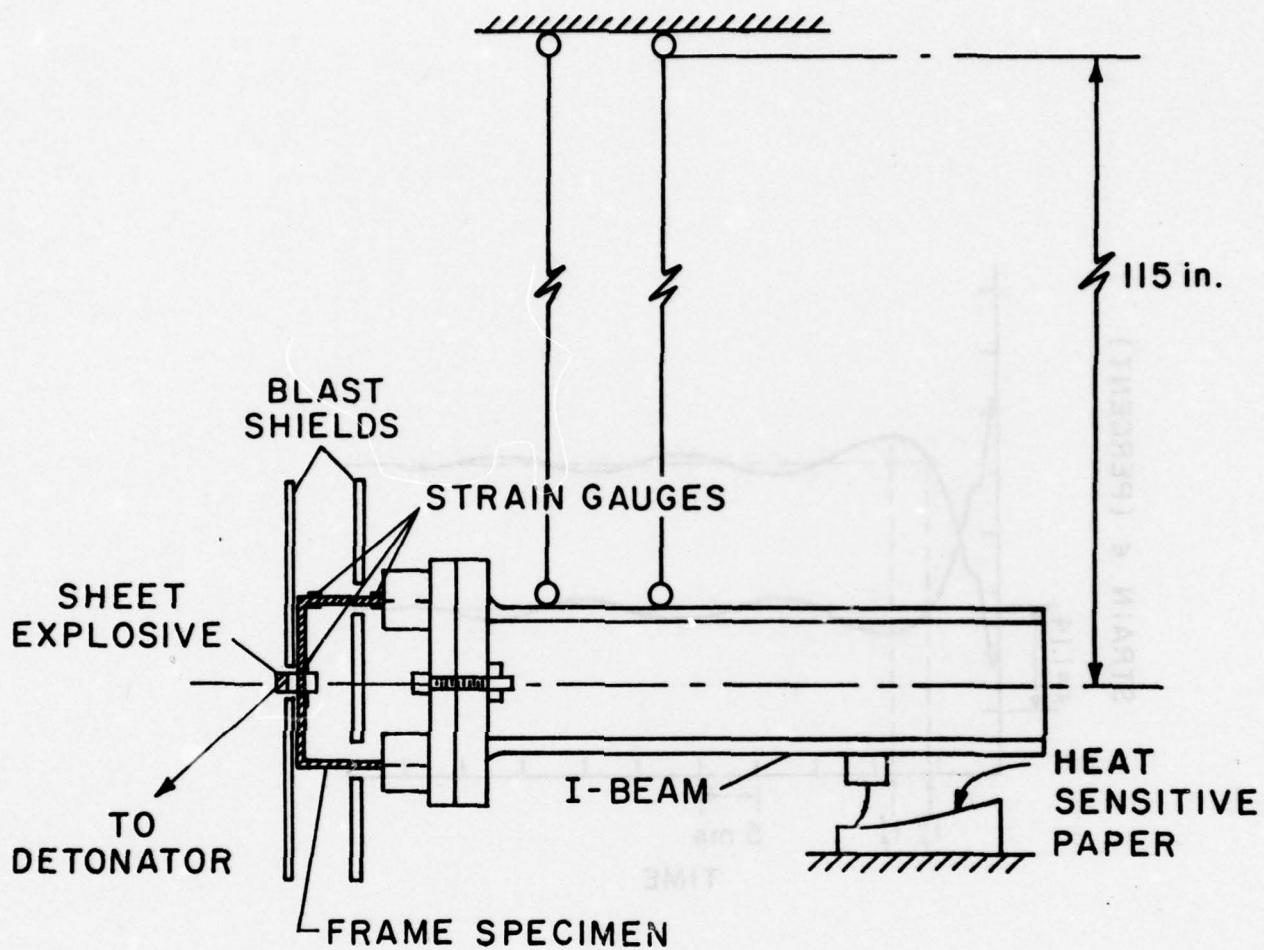
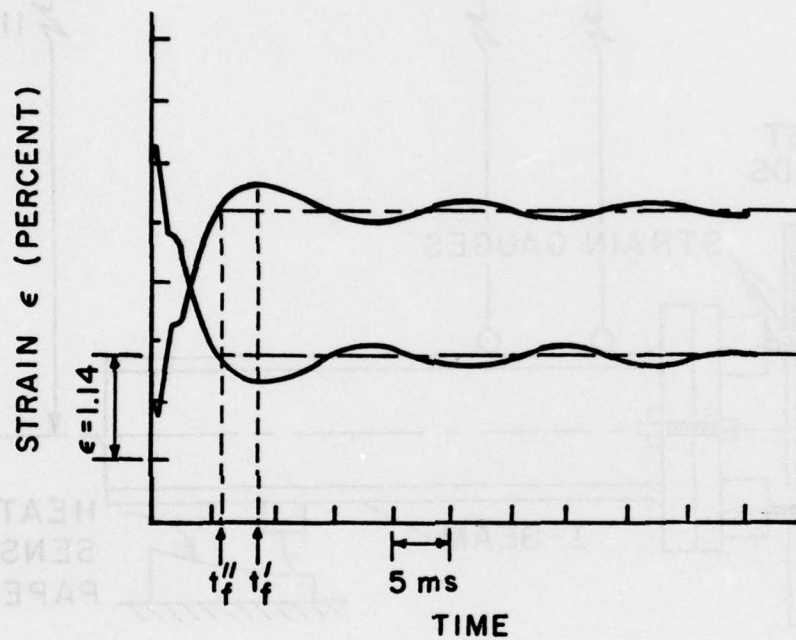


FIG. 3



STRAIN GAGES AT TOP OF COLUMN

TEST 12 STEEL FRAME

CONCENTRATED IMPULSE

FIG. 4

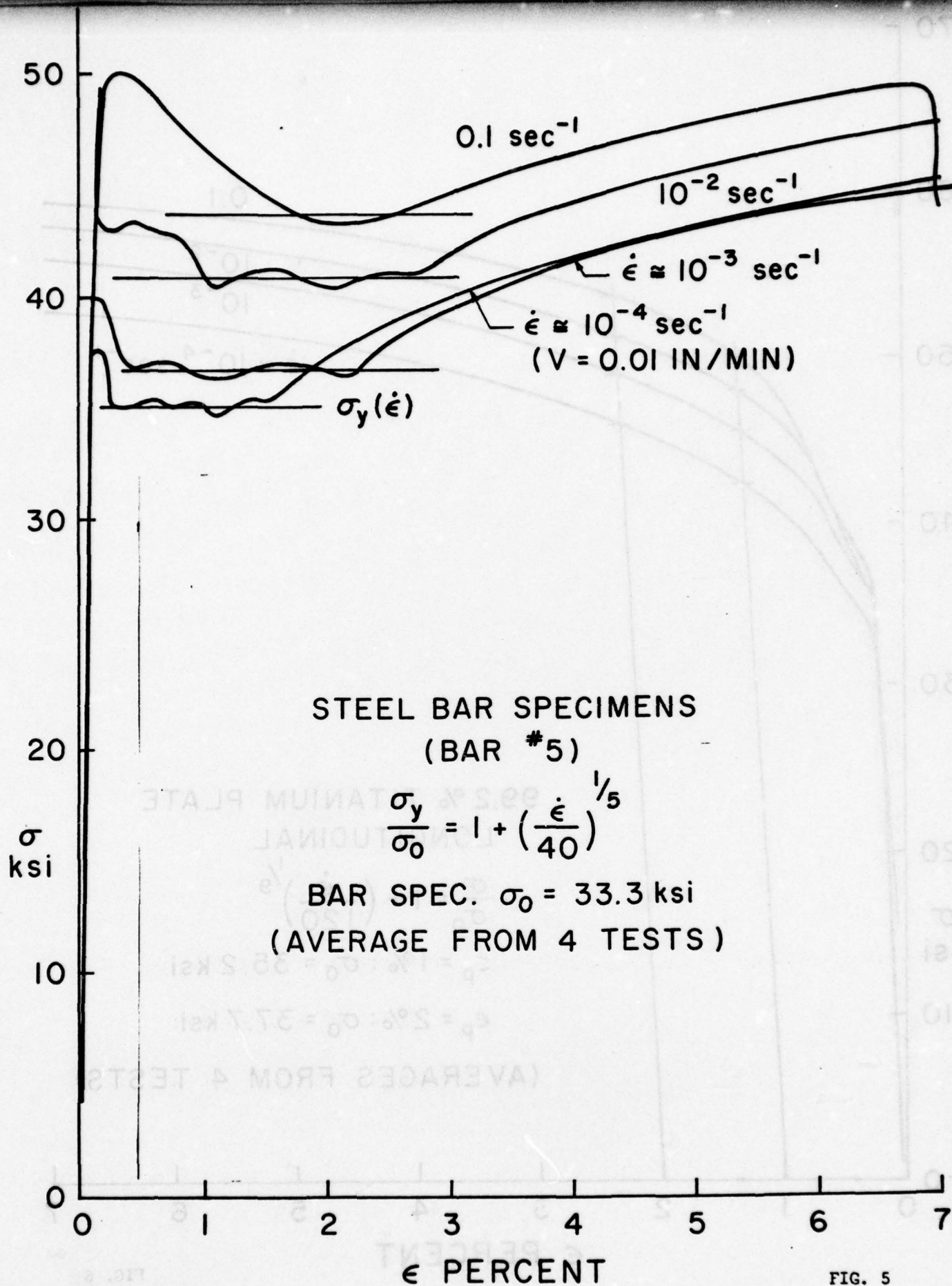


FIG. 5

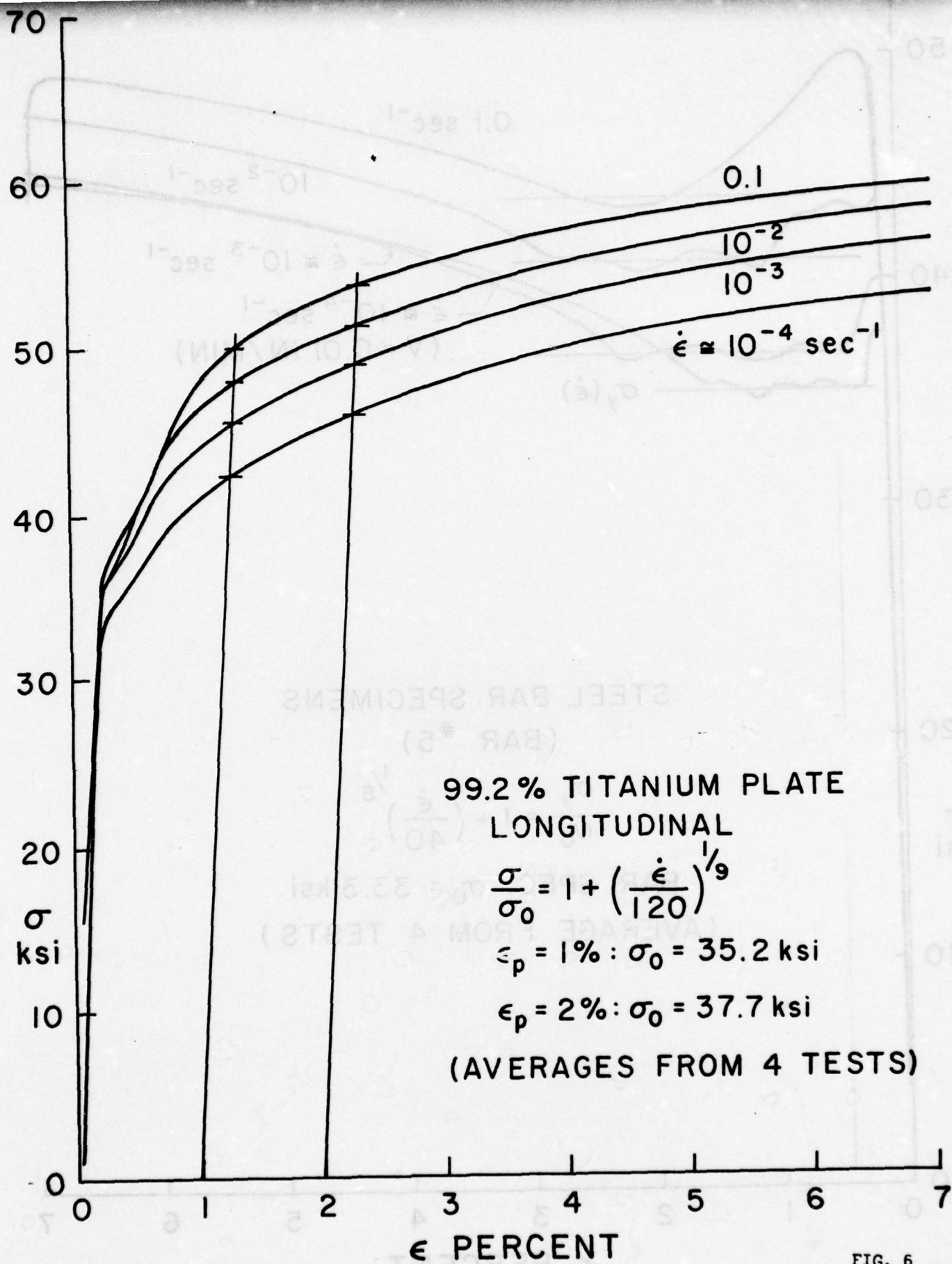


FIG. 6

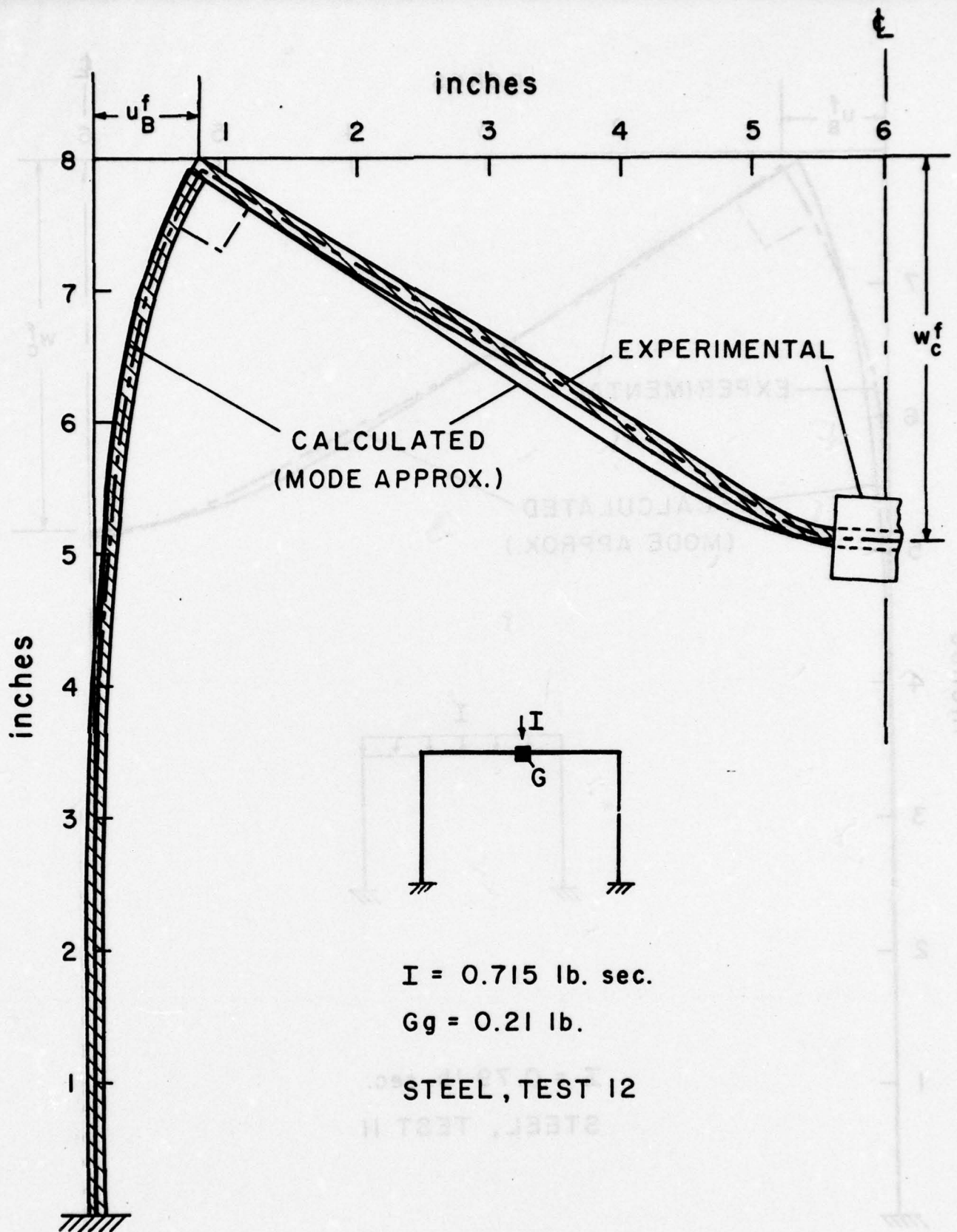


FIG. 7

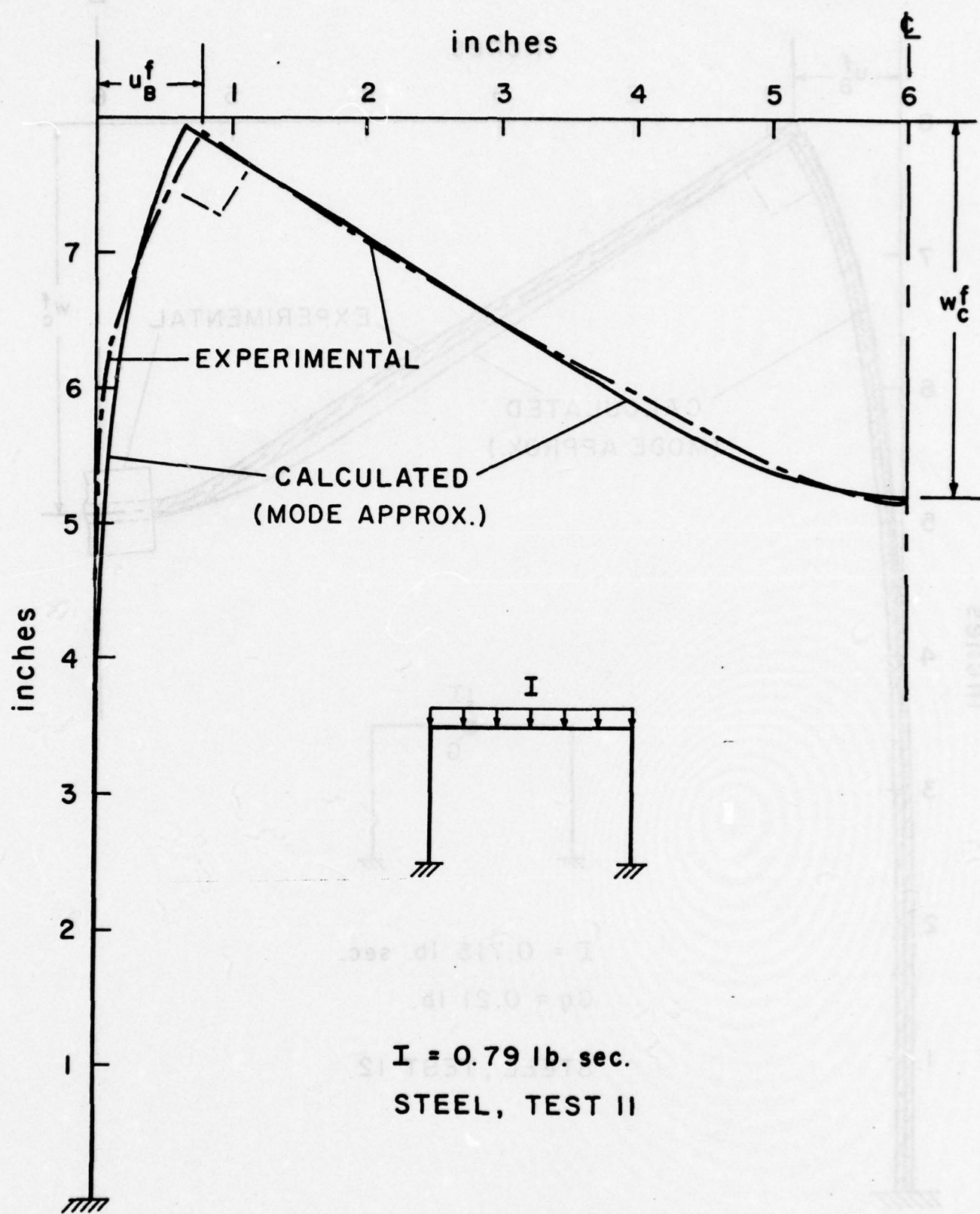


FIG. 8

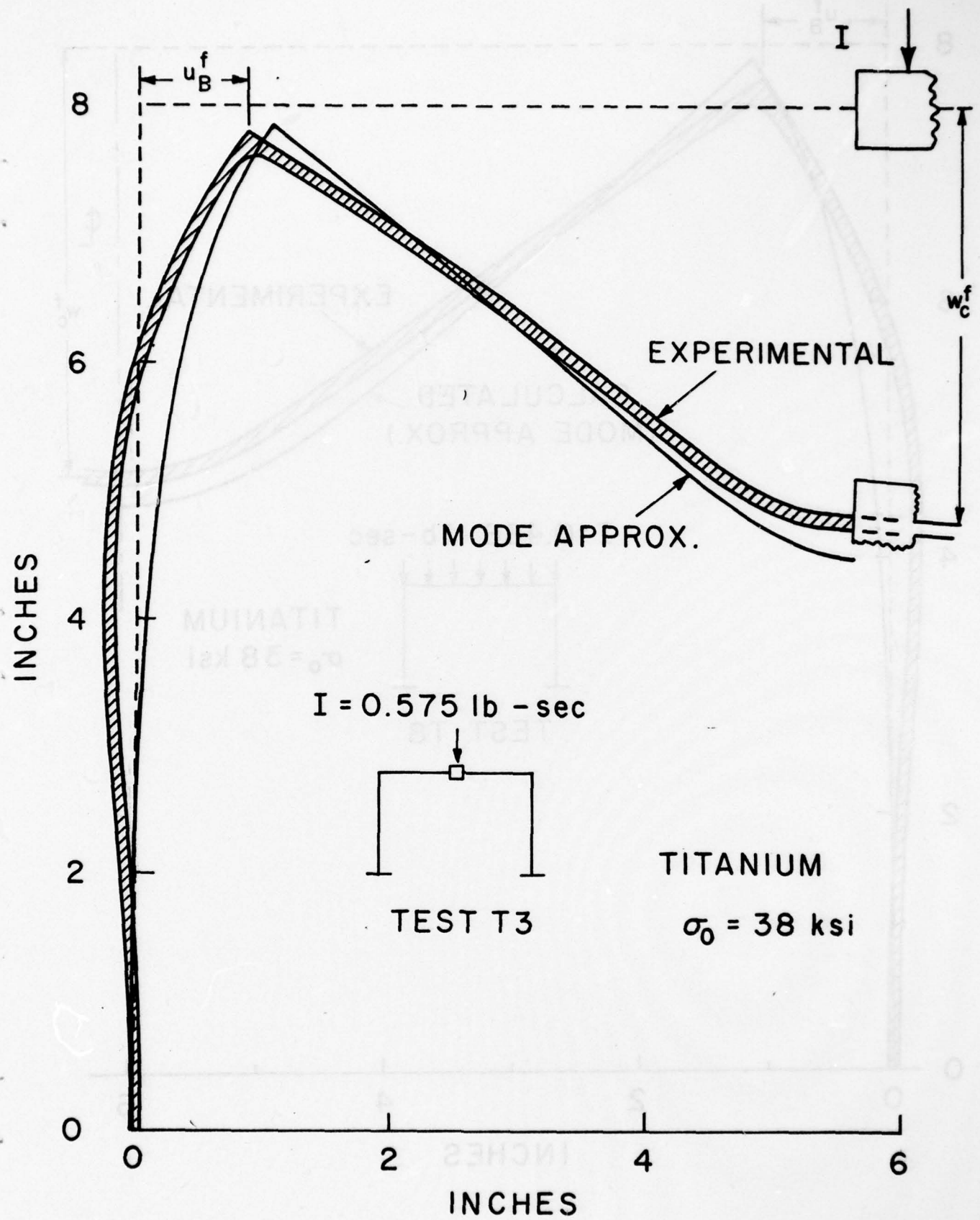


FIG. 9

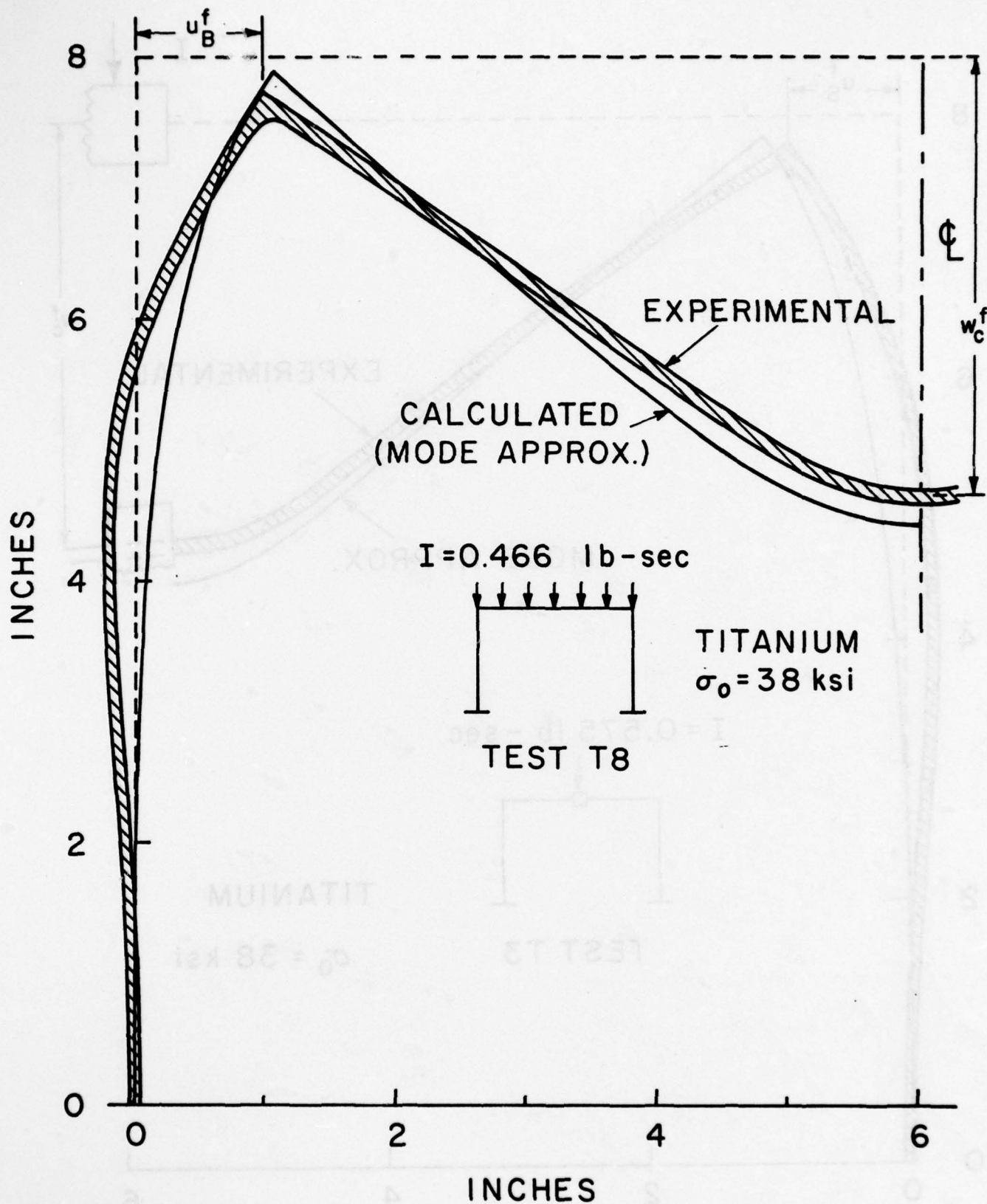


FIG. 10

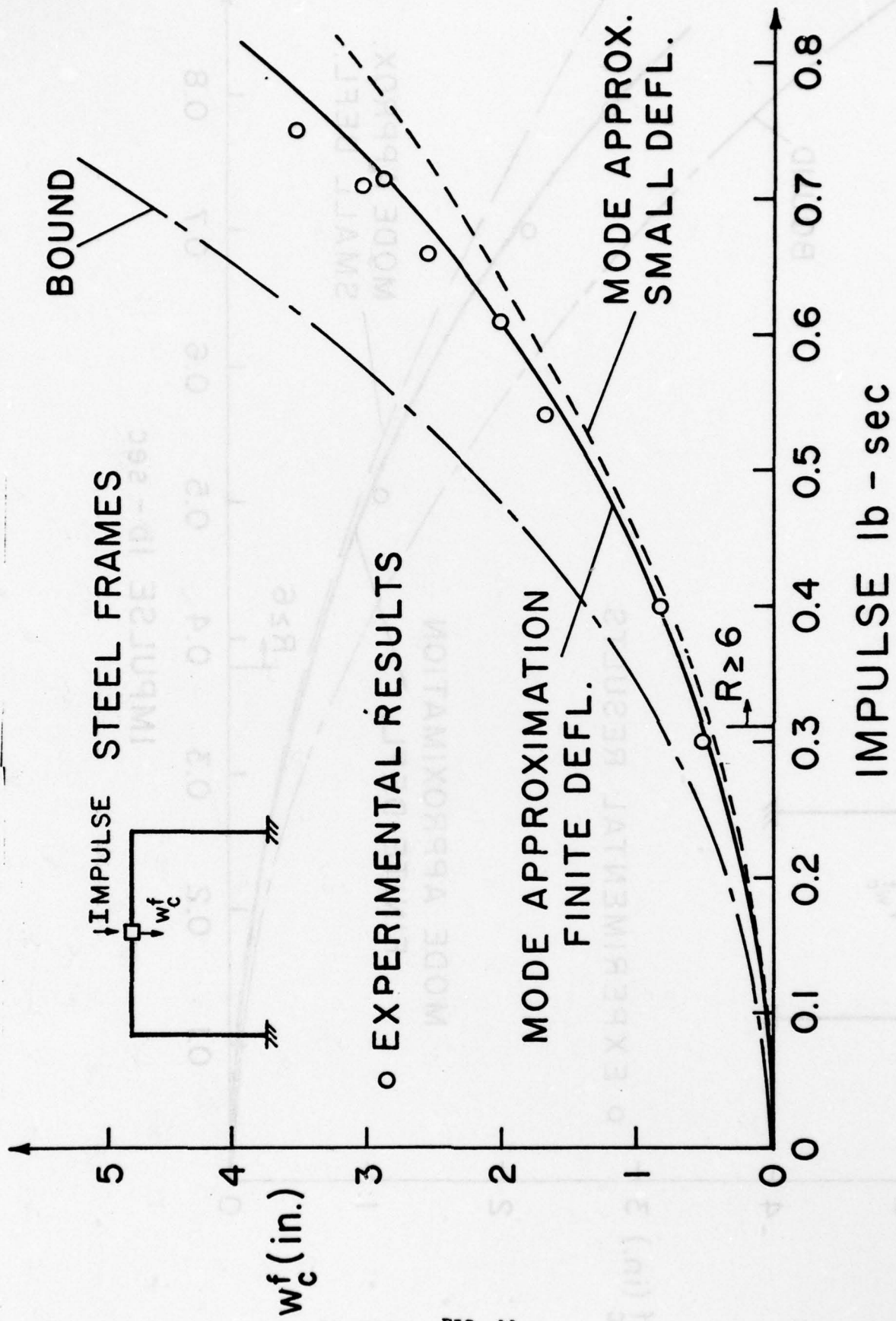


FIG. 11

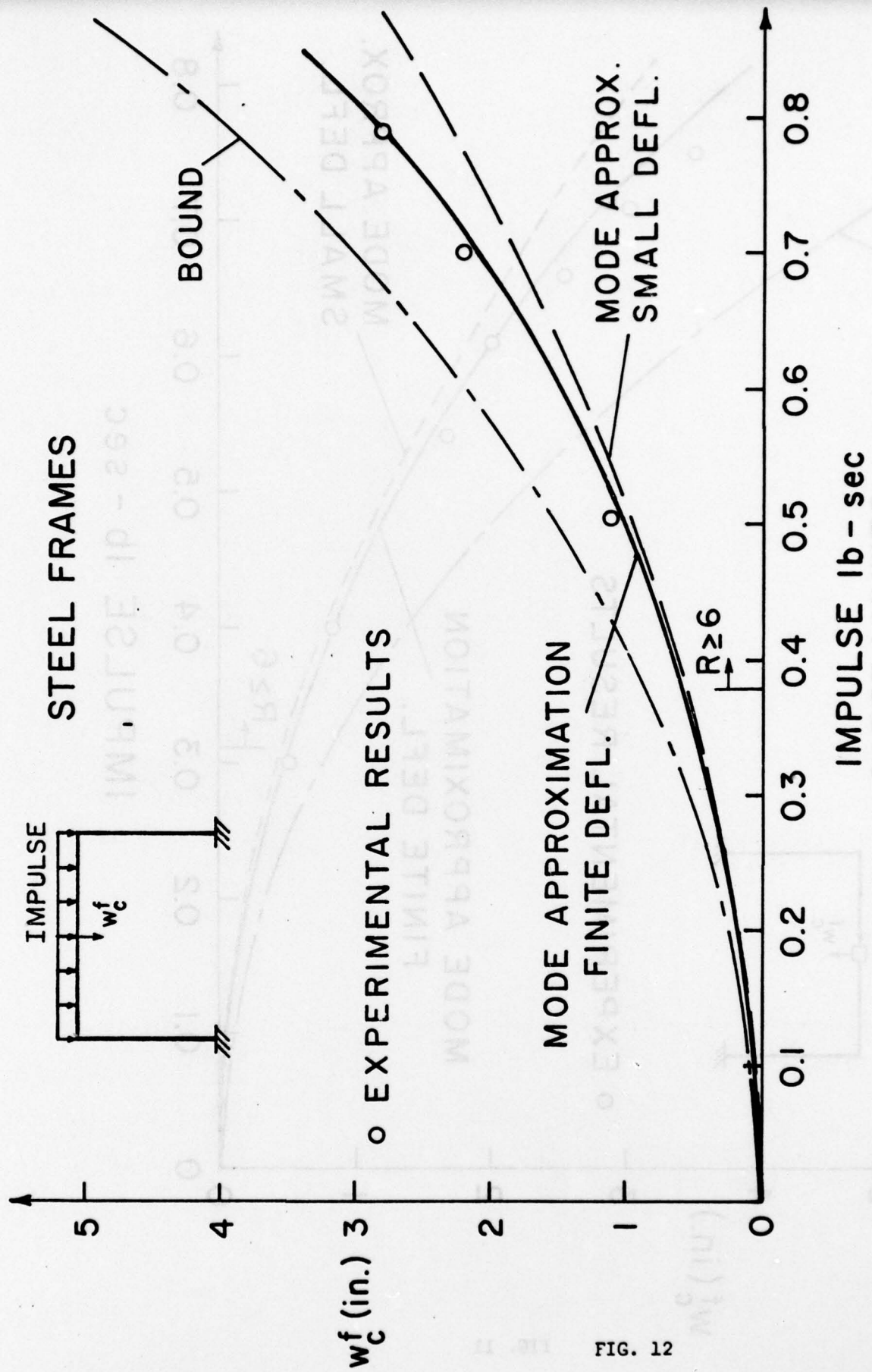


FIG. 12

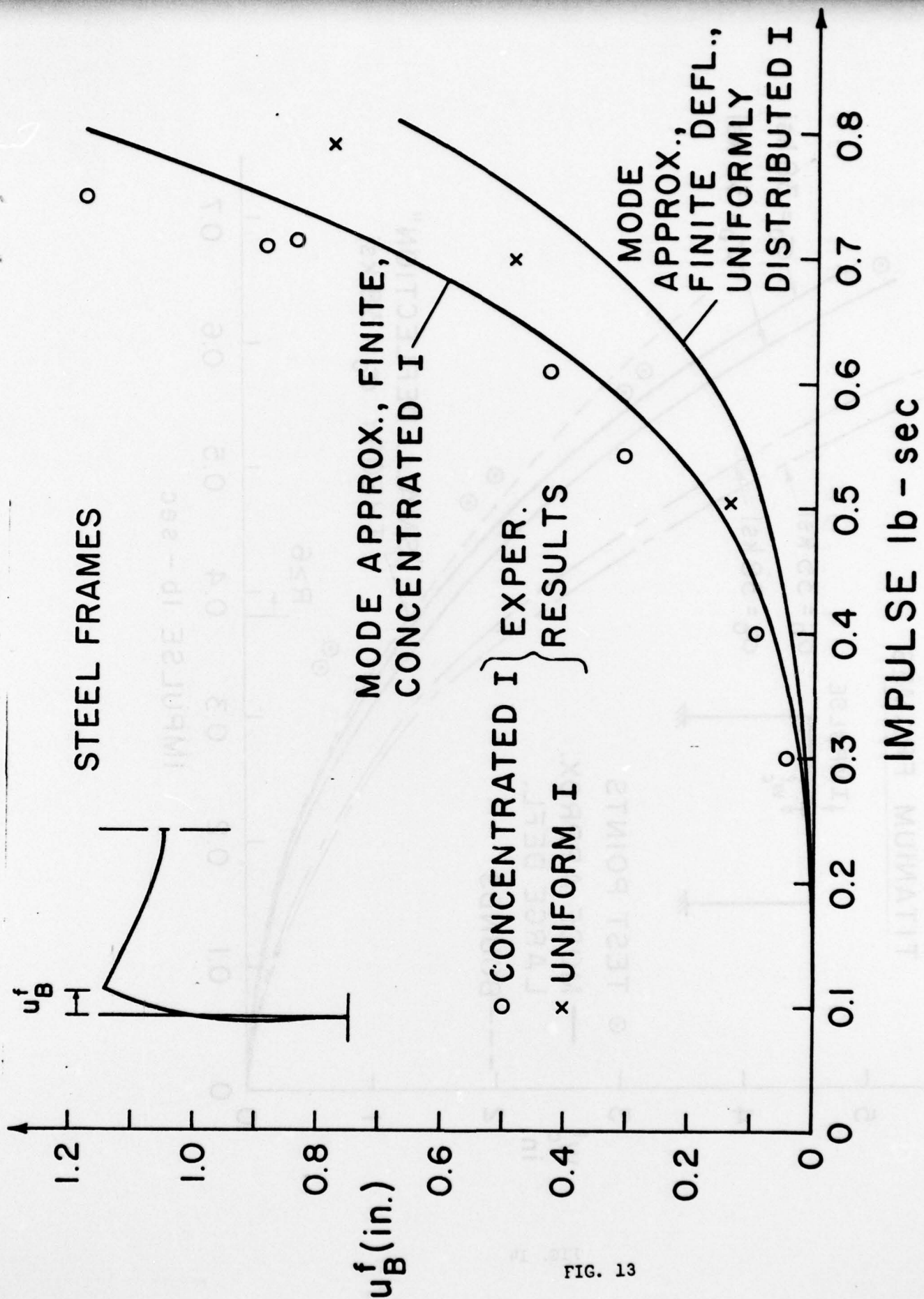


FIG. 13

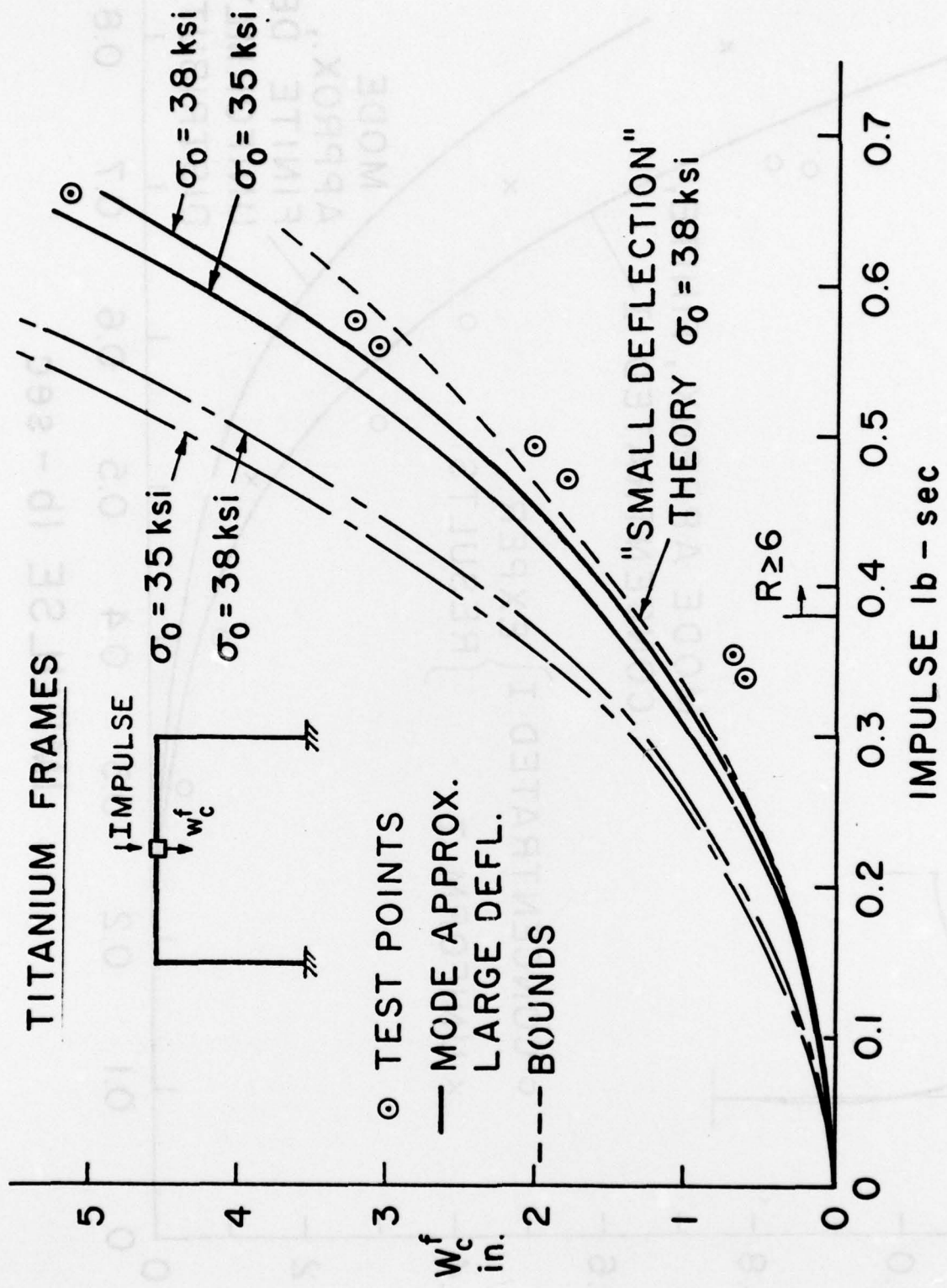


FIG. 14

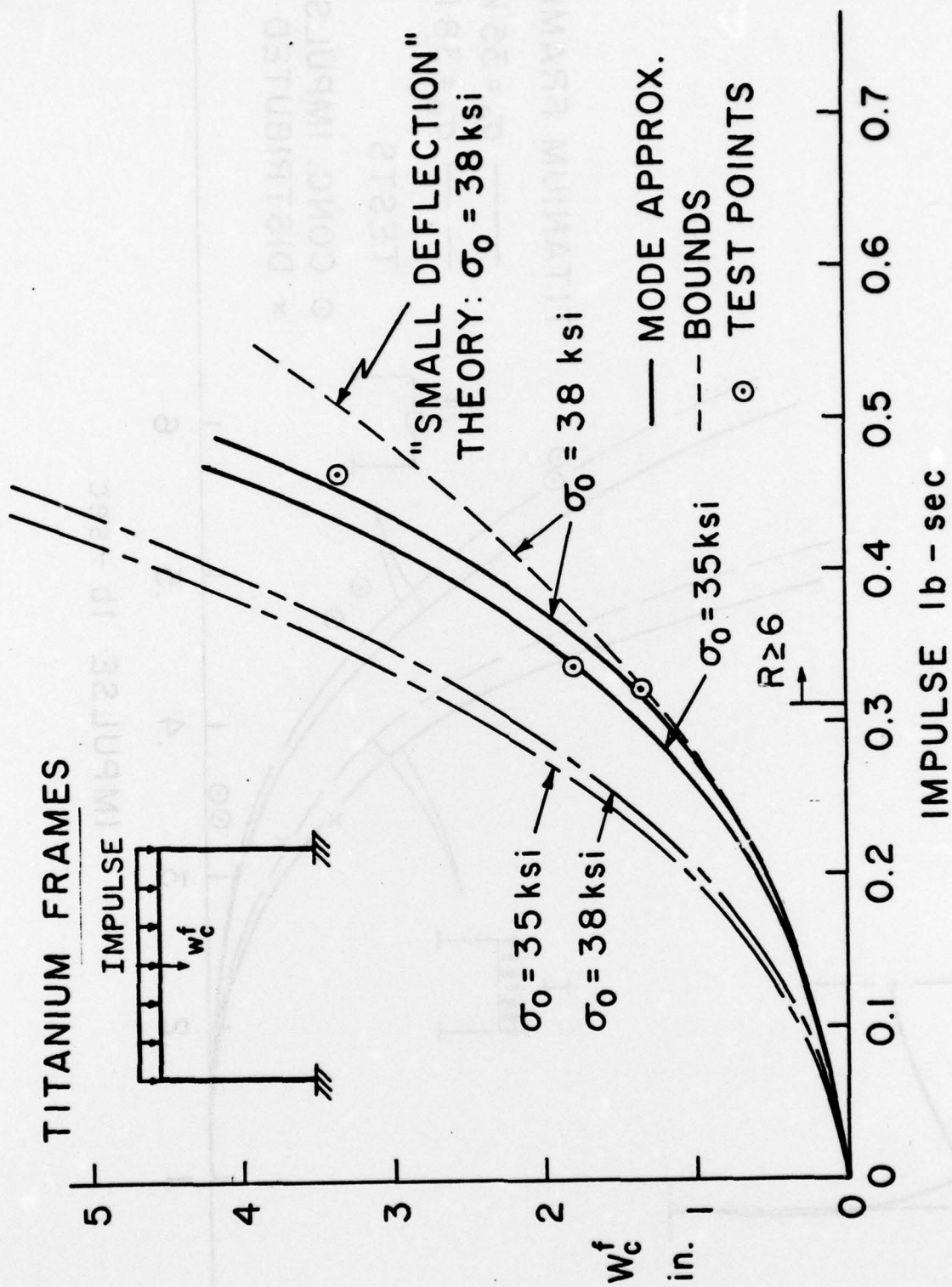


FIG. 15

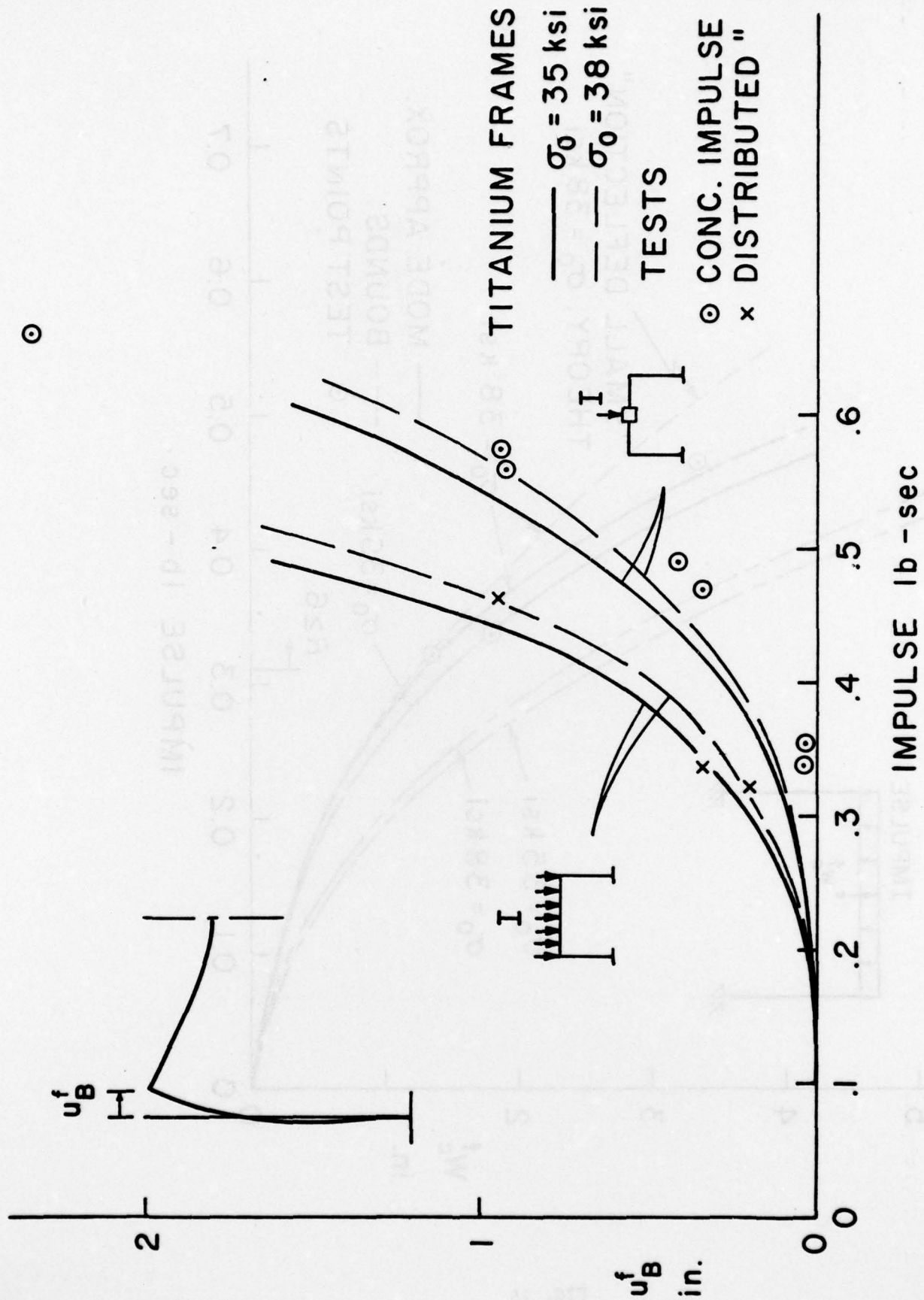


FIG. 16

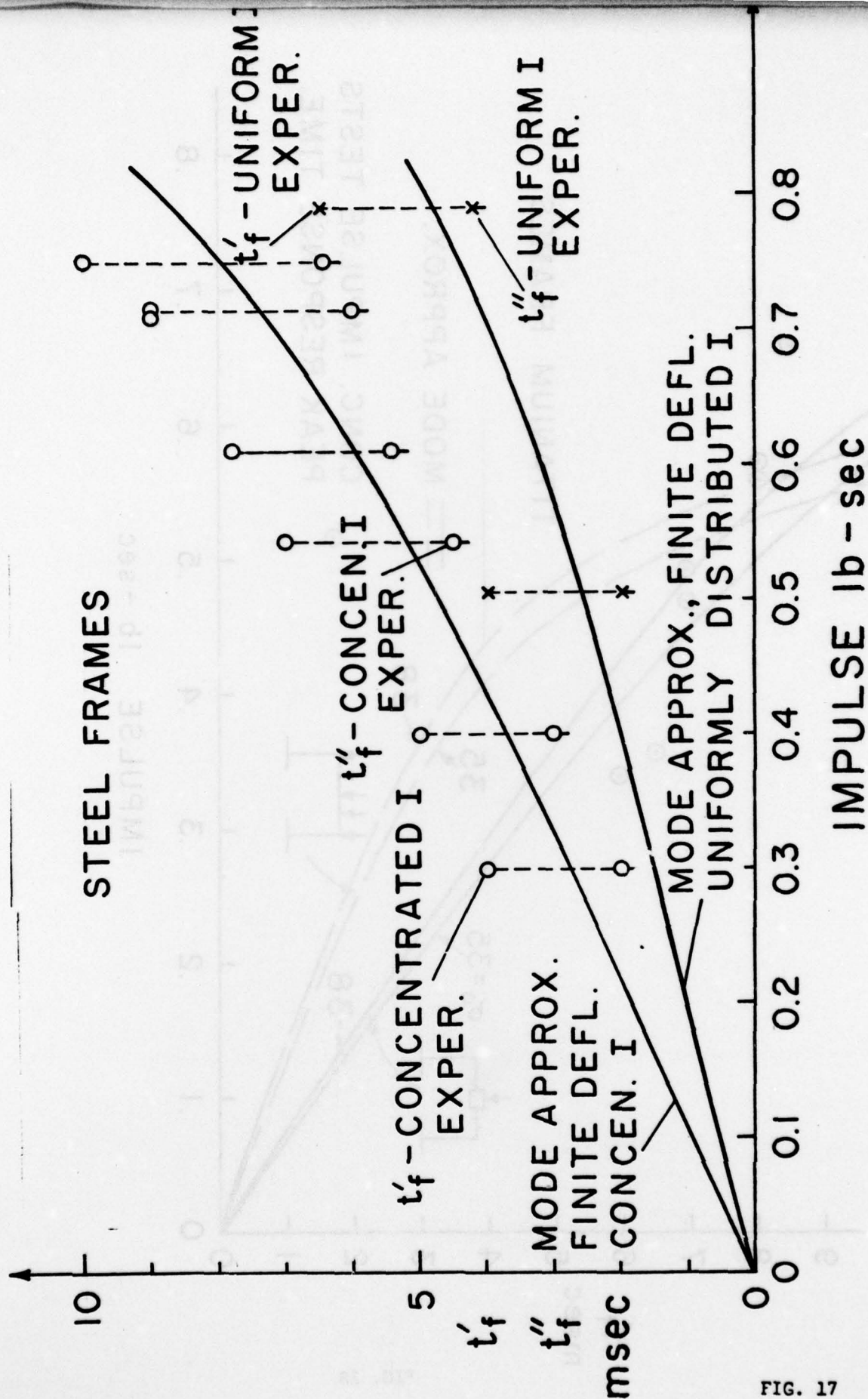


FIG. 17

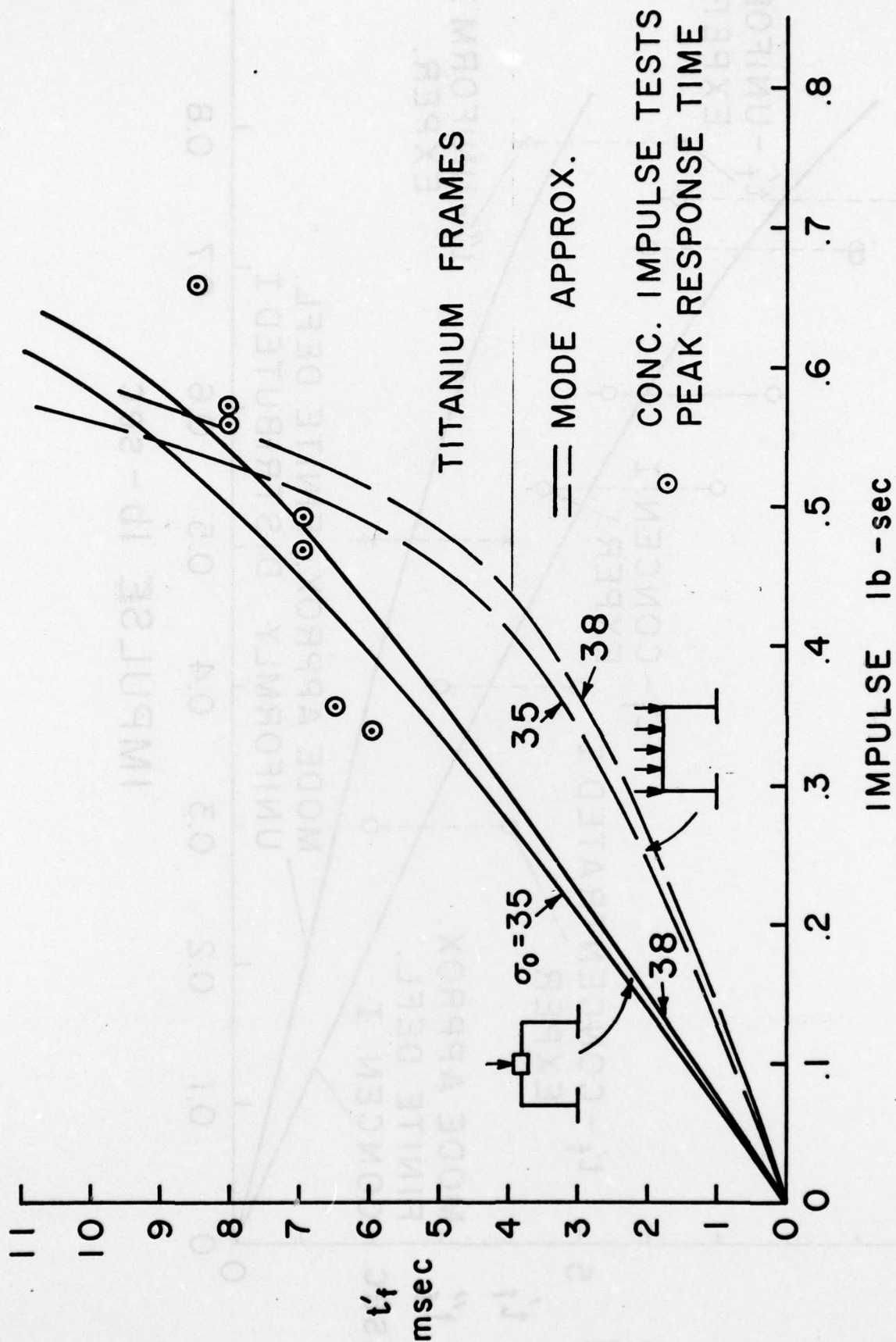


FIG. 18

Appendix

The elements of the mode approximation technique are here summarized as background for the discussion of test results in the text. The basic concept of the mode technique is that a complete solution is obtained in mode form, i.e., with velocity and acceleration vectors written as

$$\dot{\mathbf{u}}_i^*(\mathbf{x}, t) = T(t) \phi_i(\mathbf{x}) \quad (\text{A1a})$$

$$\ddot{\mathbf{u}}_i^*(\mathbf{x}, t) = \dot{T}(t) \phi_i(\mathbf{x}) \quad (\text{A1b})$$

where $T(t)$ is a scalar function of time and $\phi_i(\mathbf{x})$ is a vector-valued function of space variables. This is supposed to satisfy all the field equations of the structure (dynamics, kinematics, material behavior, and boundary fixing conditions). In a problem of impulsive loading, the initial velocity distribution is specified as $\dot{\mathbf{u}}_i^0(\mathbf{x})$. The initial field of the mode solution (A1) does not agree with this in general, $\phi_i(\mathbf{x})$ being determined by the geometry and material of the structure. The initial magnitude $T(0) = T_0$ can be chosen so as to minimize the difference between the two initial velocity fields, as defined by

$$\Delta^0(\dot{\mathbf{w}}_i^0) = \Delta[\dot{\mathbf{u}}_i^0(\mathbf{x}) - \dot{\mathbf{u}}_i^{*0}(\mathbf{x})] = \frac{1}{2} \int_V \rho (\dot{\mathbf{u}}_i^0 - T_0 \phi_i)(\dot{\mathbf{u}}_i^0 - T_0 \phi_i) dV \quad (\text{A2})$$

where ρ is the mass density and the integral extends over the structure.

Since $\dot{\mathbf{u}}_i^0(\mathbf{x})$ is specified and $\phi_i(\mathbf{x})$ is a property of the structure, Δ^0 is a function of T_0 ; minimization of Δ^0 gives the result

$$T_0 = \frac{\int_V \rho \dot{\mathbf{u}}_i^0 \phi_i dV}{\int_V \rho \phi_i \phi_i dV} \quad (\text{A3})$$

Δ^0 is the initial value of the functional

$$\Delta(t) = \frac{1}{2} \int_V \rho (\dot{u}_i - \dot{u}_i^*)(\dot{u}_i - \dot{u}_i^*) dV \quad (A4)$$

For a wide class of plastic behavior¹ $\Delta(t)$ is a non-increasing function of time. The two solutions (actual and mode form) converge, and when the initial amplitude T_0 is chosen according to Eq. (A3), in many cases they become identical. Hence the error in the final principal deflection is generally much less than the difference between initial velocity magnitudes.²

For the concentrated impulse tests, the initial velocity field is taken as a velocity V_0 of the attached mass, the rest of the frame being at rest; while in the tests with distributed impulse, the beam member is assumed to have uniform velocity V_0 . These are related to the measured impulse I by

$$V_0 = \frac{I}{G} ; \quad V_0 = \frac{I}{2\rho bHL_1} \quad (A5a, b)$$

where G is the mass of the attached block, ρ is mass density, and b, H, L_1 are the width, thickness, and half-span, respectively of the beam member. The mode form solution is written for the frame problems as

$$\frac{\tau}{H} \dot{w} = \dot{w}_*(t) \phi_1(x) \quad (A6a)$$

$$\frac{\tau}{H} \dot{u} = \dot{w}_*(t) \phi_2(x) \quad (A6b)$$

¹Martin, J. B., "A Note on Uniqueness of Solutions for Dynamically Loaded Rigid-Plastic and Rigid-Viscoplastic Continua," J. Appl. Mech., Vol. 33, pp. 207-209, 1966.

²Martin, J. B., and Symonds, P. S., "Mode Approximations for Impulsively Loaded Rigid-Plastic Structures," J. Eng. Mech. Div., Proc. ASCE, Vol. 92, pp. 43-66, 1966.

where \dot{w}_* is the mode velocity amplitude, here taken as the velocity of the midpoint of the beam member, so that the integral w_* is the displacement of this point; these are dimensionless, using $\tau = \sqrt{\rho b H^2 L_1 / M_0} = 2L_1 \sqrt{\rho / \sigma_0}$ and H as reference time and length magnitudes, respectively. The notation for components is shown in Fig. A1, and this figure also illustrates the initial shape function ϕ_1 in the beam member. When the "matching" equation (A3) is written in terms of dimensionless velocities, and combined with Eqs. (A5), we obtain the following relations:

$$\begin{array}{l} \text{Concentrated} \\ \text{Impulse} \end{array} \quad \frac{\dot{w}_*^0}{\dot{w}_c^0} = \frac{k}{\int_0^1 \phi_1^2 dx + k} ; \quad \frac{I}{\dot{w}_*^0} = b H^2 \sqrt{\rho \sigma_0} \left[\int_0^1 \phi_1^2 dx + k \right] \quad (\text{A7a})$$

$$\begin{array}{l} \text{Distributed} \\ \text{Impulse} \end{array} \quad \frac{\dot{w}_*^0}{\dot{w}_c^0} = \frac{\int_0^1 \phi_1 dx}{\int_0^1 \phi_1^2 dx} ; \quad \frac{I}{\dot{w}_*^0} = b H^2 \sqrt{\rho \sigma_0} \frac{\int_0^1 \phi_1^2 dx}{\int_0^1 \phi_1 dx} \quad (\text{A7b})$$

where $\phi_1(x)$, $0 \leq x \leq 1$, is the initial shape function for transverse velocities in part BC of the beam member, $k = G/2L_1 \rho b H$, and b, H, ρ, σ_0 are specimen properties, Table 1.

The integration of the equations to obtain the mode form response, taking account of finite deflections through "von Karman type" (rotation) terms, is discussed in [2]. The equations in nondimensional form contain as input parameters the initial mode velocity amplitude \dot{w}_*^0 , the mass ratio k , length ratios defining the structure geometry, and two quantities involving material properties, namely

$$n ; \quad \alpha = \frac{4L_1^2 \dot{\epsilon}_0^2 \tau}{H^2} = \frac{8L_1^3}{H^2} \dot{\epsilon}_0 \sqrt{\frac{\rho}{\sigma_0}} \quad (\text{A8})$$

where $n, \dot{\epsilon}_0, \sigma_0$ express strain rate dependent behavior as used in Eq. (2). Integration of the mode equations then furnishes final dimensionless displacements and response durations as

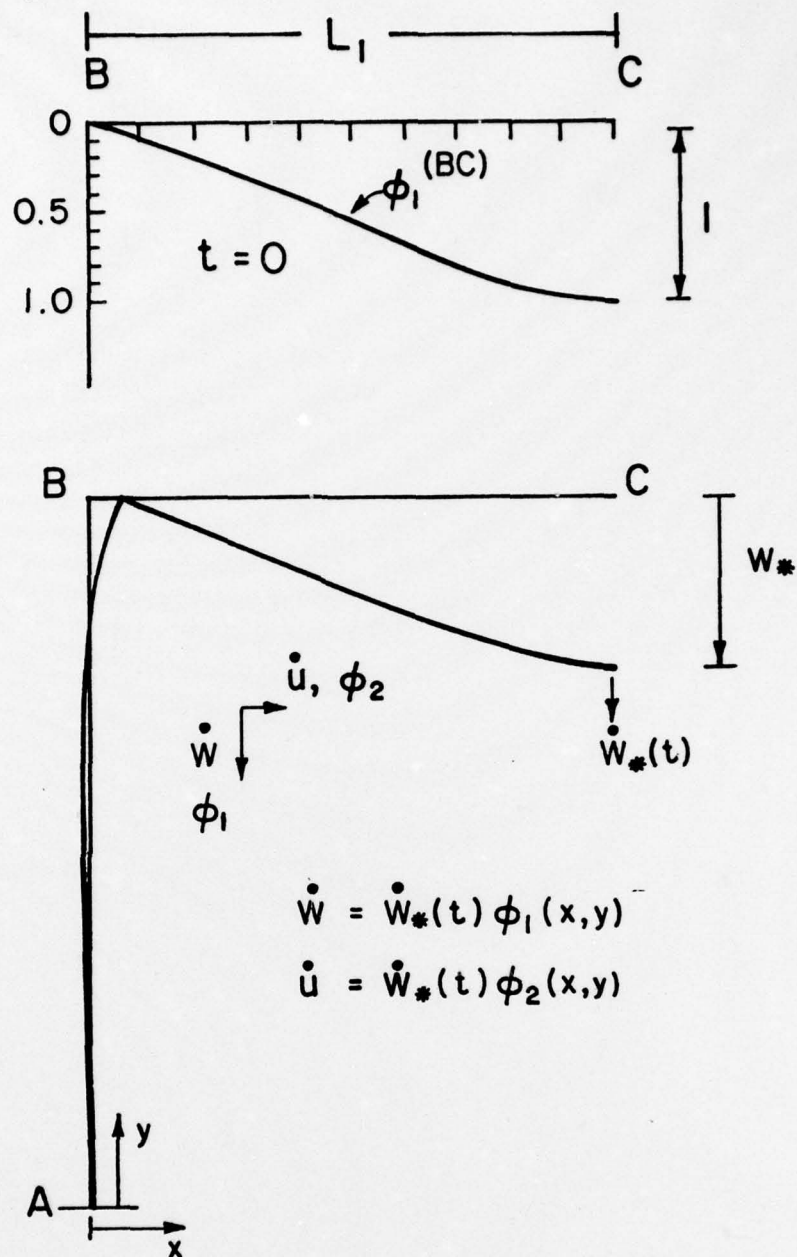
$$w_{*}^f = F_1(\dot{w}_{*}^o, \alpha, n, \frac{L_1}{H}, \frac{L_1}{L_2}, k) \quad (A9a)$$

$$t_f = F_2(\dot{w}_{*}^o, \alpha, n, \frac{L_1}{H}, \frac{L_1}{L_2}, k) \quad (A9b)$$

The physical quantities are obtained by multiplying these respectively by H and $\tau = 2L_1\sqrt{\rho/\sigma_0}$. Equations (A7) furnish the corresponding impulse in physical units.

In general the dependence of the mode response on the material properties is through the parameters n and α , Eqs. (A8). The dependence on α , however is quite weak. If viscoplastic behavior is treated by constitutive equations of homogeneous viscous form [8], this parameter appears only in the form $\alpha^{1/vn}$ where v is a factor depending on strain rate of the order of 2.

Alternative values of quantities such as σ_0 can often be considered simply by making the corresponding change in impulse I as given by Eq. (A7), disregarding the change in α . Thus a single integration of the mode equations for a representative value of α serves as a sort of master solution, which can be used for a number of special cases. This adds to the efficiency of the method, particularly when large deflections are being considered; for small deflections the computational work is insignificant in any case.



NOTATION FOR MODE FORM SOLUTION

FIG. A1

DOCUMENT CONTROL DATA - R & D

(Security classification of title, body of abstract and indexing annotation must be entered when the overall report is classified)

1. ORIGINATING ACTIVITY (Corporate author) Division of Engineering, Brown University Providence, RI 02912		2a. REPORT SECURITY CLASSIFICATION Unclassified	
		2b. GROUP	
3. REPORT TITLE Experiments on Dynamic Plastic Loading of Frames			
4. DESCRIPTIVE NOTES (Type of report and inclusive dates) Technical Report			
5. AUTHOR(S) (First name, middle initial, last name) Sol R. Bodner Paul S. Symonds			
6. REPORT DATE July 1977		7a. TOTAL NO. OF PAGES 38	7b. NO. OF REFS 11
8a. CONTRACT OR GRANT NO. N00014-75-C-0860 ✓ b. PROJECT NO. ENG74-21258		9a. ORIGINATOR'S REPORT NUMBER(S) N00014-0860/4 ✓	
c. d.		9b. OTHER REPORT NO(S) (Any other numbers that may be assigned this report)	
10. DISTRIBUTION STATEMENT <div style="border: 1px solid black; padding: 5px; text-align: center;">DISTRIBUTION STATEMENT A Approved for public release; Distribution Unlimited</div>			
11. SUPPLEMENTARY NOTES		12. SPONSORING MILITARY ACTIVITY Office of Naval Research	
13. ABSTRACT Tests are described on plane frames of mild steel and titanium (commercial purity) in which high intensity short duration pressure pulses were applied transversely to the beam member either uniformly over this member or concentrated at its center. The objective was to examine applications of two estimation techniques (upper bounds on deflections and the mode approximation technique) for major response features of pulse loaded structures at large deflections, taking account of strong plastic strain rate sensitivity. Loads over a range such as to cause final deflections up to about a third of the span were applied by detonating explosive sheet. Agreement between estimated and measured final deflections was often very good (generally conservative) but the intrinsic error of the mode technique was not observed as expected. ↑			

14.	KEY WORDS	LINK A		LINK B		LINK C	
		ROLE	WT	ROLE	WT	ROLE	WT
	plane frames						
	impulsive loading						
	plastic deformation						
	tests						
	approximation techniques						